symmetry

MDPI

Article

Maximum Principles for Fractional Diffusion Problems

Stanislav Harizanov and Svetozar Margenov *

Institute of Information and Communication Technologies, Bulgarian Academy of Sciences and Centre of Excellence in Informatics and Information and Communication Technologies, 1113 Sofia, Bulgaria; sharizanov@parallel.bas.bg

* Correspondence: margenov@parallel.bas.bg

Abstract

The maximum principle is a widely used qualitative property of linear (and not only) elliptic boundary value problems. A natural goal for developing numerical methods is for the approximate solution to have a similar property. In this case, we say that a discrete maximum principle holds. In many cases, such a requirement is critical to ensuring the reliability of computational models. Here, we consider multidimensional linear elliptic problems with diffusion and reaction terms. Such problems have been studied and analyzed for many decades. Since relatively recently, scientists have faced conceptually new challenges when considering anomalous (fractional) diffusion. In the present paper, we concentrate on the case of spectral fractional diffusion. Discretization was carried out using the finite difference method and the finite element method with a lumped mass matrix. In large-scale multidimensional problems, the computational complexity of dense matrix operations is critical. To overcome this problem, BURA (best uniform rational approximation) methods were applied to find the efficient numerical solutions of emerging dense linear systems. Thus, along with the need to satisfy the discrete maximum principle associated with the mesh method applied for discretization of the differential operator, the issue of the monotonicity of BURA numerical solution arises. The presented results are threefold and include the following: (i) maximum principles for fractional diffusion–reaction problems; (ii) sufficient conditions for discrete maximum principles; and (iii) sufficient conditions for monotonicity of the investigated BURA- or BURA-like approximation methods. A novel, systematic theoretical analysis is developed for sub-diffusion with a fractional power $\alpha \in (1/2, 1)$ and a constant reaction coefficient. The theoretical findings are further supported by numerical examples.

Keywords: maximum principle; non-negativity preserving; fractional diffusion; rational approximation

Check for updates

Academic Editor: Francisco Martinez

Received: 27 December 2025
Revised: 27 January 2026
Accepted: 30 January 2026
Published: 31 January 2026

Copyright: © 2026 by the authors. Licensee MDPI, Basel, Switzerland. This article is an open access article distributed under the terms and conditions of the Creative Commons Attribution (CC BY) license.

1. Introduction

1.1. Motivation

The maximum principle is an important qualitative property of the solution of second-order elliptic boundary value problems. This is one of the most useful approaches applied for solving a wide range of problems in the study of partial differential equations over the years. A basic fact of calculus is that if a function has a positive second derivative on a given interval, then it can only attain its maximum at the end points of that interval. Essentially, the same idea applies to partial differential equations. The theory of the maximum principle for second-order differential equations is well developed, including,

for example, the cases of linear convection–diffusion–reaction problems, elliptic systems, as well as generalizations to quasilinear equations; see, e.g., [1–7]. In this paper, we consider multidimensional diffusion–reaction boundary value problems. The present study is motivated by the challenges when standard (local) diffusion is replaced by anomalous (non-local) diffusion.

Let $\Omega \subset \mathbb{R}^d$, $d \in \{2,3\}$, be a bounded Lipschitz domain, where $\partial\Omega$ is a polygonal/polyhedral boundary. Also, let $\mathbf{a}(x)$ be a $d \times d$ symmetric and positive definite (SPD) coefficient matrix that is uniformly bounded in Ω. We consider the bilinear form on $V \times V$

$$A(w,v) := \int_\Omega \big(\mathbf{a}(x)\nabla w(x) \cdot \nabla v(x)\big)dx, \tag{1}$$

where $V := \{v \in H^1(\Omega) : \ v(x) = 0 \text{ on } \partial\Omega\}$. We denote by $\mathcal{A}$ the self-adjoint and positive definite diffusion operator defined by the bilinear form (1). We begin by considering the diffusion–reaction operator $\mathcal{A} + q$, where the constant $q \geq 0$ is a reaction coefficient.

As is known, the maximum principle applies to the diffusion–reaction problem. Given the formulation above, it is equivalent to the following statement: suppose that $\mathcal{A}u(x) + qu(x) \geq 0$ in Ω, then $u(x) \geq 0$ for every $x \in \Omega$. This is why we say that the operator preserves non-negativity. Preserving the maximum principle in the discrete model is one of the main requirements for numerical methods. In this study, we consider a $(2d+1)$-point finite difference stencil or a linear finite element discretization. The discrete maximum principle is valid if from $(\mathbb{A} + q\mathbb{I})\mathbf{u} \geq 0$ it follows that $\mathbf{u} \geq 0$. In the finite difference case, $\mathbb{A}$ is the matrix arising from the discretization of the diffusion operator, $\mathbb{I}$ is the identity matrix, and $\mathbf{u}$ is the vector of nodal unknowns. A similar representation applies in the finite element case if the standard matrix equation is multiplied by $\mathbb{M}^{-1}$, leading to $\mathbb{A} = \mathbb{M}^{-1}\mathbb{S}$, where $\mathbb{S}$ and $\mathbb{M}$ are the stiffness and mass matrices, respectively. Here, as everywhere else where the context implies, the inequalities are in a pointwise sense. Sufficient conditions for the mesh under which this discrete maximum principle holds are known.

There are several non-equivalent definitions of fractional diffusion. We will consider the case of the spectral fractional diffusion (sub-diffusion when $\alpha \in (0,1)$) operator associated with the bilinear form (1) given by

$$\mathcal{A}^\alpha u(x) = \sum_{i=1}^{\infty} \lambda_i^\alpha c_i \psi_i(x), \text{ where } u(x) = \sum_{i=1}^{\infty} c_i \psi_i(x). \tag{2}$$

Here, $\{\psi_i(x)\}_{i=1}^\infty$ are the eigenfunctions of $\mathcal{A}$, orthonormal in L^2-inner product and $\{\lambda_i\}_{i=1}^\infty$ are the corresponding eigenvalues that are real and positive.

After introducing the operator $\mathcal{A}^\alpha$, we are ready to define the spectral fractional diffusion–reaction equation studied in this paper:

$$\mathcal{A}^\alpha u(x) + qu(x) = f(x), \quad x \in \Omega, \tag{3}$$

where $\Omega \subset \mathbb{R}^d$, $d \in \{2,3\}$ is a bounded Lipshitz domain with a polygonal/polyhedral boundary $\partial\Omega$, $\alpha \in (1/2,1)$, $q > 0$ is a constant, and $f(x) \in L^2(\Omega)$ is a given function.

The finite difference method (FDM) and finite element method (FEM) are employed for discretization. Then, in the discrete setting, the symmetric and positive definite matrix $\mathbb{A} \in \mathbb{R}^{N\times N}$ represents the diffusion operator. Its spectral decomposition is given by

$$\mathbb{A} = \mathbb{W}\mathbb{D}\mathbb{W}^T,$$

where $\mathbb{W}$ is the matrix whose columns are the eigenvectors of $\mathbb{A}$ and $\mathbb{D}$ is the diagonal matrix containing the corresponding eigenvalues. The fractional power of $\mathbb{A}$ is then defined by

$$\mathbb{A}^{\alpha} = \mathbb{W}\mathbb{D}^{\alpha}\mathbb{W}^{T},$$

In the case of finite element discretization, the eigenpairs are obtained by solving the generalized eigenvalue problem $\mathbb{S}\Psi = \lambda\mathbb{M}\Psi$.

In the following sections, the interrelated maximum principles for fractional diffusion–reaction problems and the corresponding discrete maximum principles will be investigated. The fractional diffusion matrix is dense. Thus, along with the need to satisfy the discrete maximum principle, we will discuss the issue of an efficient numerical solution of such dense linear systems that preserves non-negativity.

1.2. Overview of Existing Related Results

The relationships between fractional and standard diffusion are important for understanding the qualitative and quantitative properties of the non-local operator. The spectral definition of the operator $\mathcal{A}^{\alpha}$ provides such a dependence in an explicit form. Unfortunately, the Formula (2), as well as its discrete analogue, are not very useful in the analysis, as well as in the numerical solution of multidimensional fractional diffusion problems in computational domains with general geometry. A key role in this area is played by the results in [8,9], where it is shown that the solution of the fractional diffusion problem in $\Omega \subset \mathbb{R}^d$ can be expressed by the solution of a standard (local) elliptic boundary values problem in $\Omega \times (0, \infty) \subset \mathbb{R}^{d+1}$. In our work, we use the elliptic extension in the analysis of the maximum principle and corresponding monotonicity properties.

It is known that the $(2d + 1)$-point stencil finite difference method (FDM) preserves the non-negativity of the numerical solution of diffusion–reaction problems. In the classical paper by [10], it is shown that, for the case of a scalar isotropic diffusion coefficient, the linear finite element method (FEM) satisfies the discrete maximum principle on weakly acute-angled meshes. In the general case, the discrete maximum principle is valid for Stieltjes matrices. It is also known that element stiffness matrices for isotropic problems with constant coefficients have non-positive off-diagonal coefficients if there are no obtuse angles in the finite elements. It is also important to note that if $\mathbb{A}$ is a Stieltjes matrix, then $\mathbb{A}^{\alpha}$ is also a Stieltjes matrix if $\alpha \in (0, 1)$; see [3].

There are relatively few publications that deal with topics that are directly related to our research. Among them, we would like to mention [11], which studied strong maximum principles for fractional elliptic and parabolic problems with mixed boundary conditions. The authors use the integral definition of the fractional Laplacian, where the boundary conditions are over the entire domain $\mathbb{R}^d \setminus \Omega$. We note that this is a conceptually different task, and the obtained results and approaches cannot be applied to the case of spectral fractional diffusion.

Most likely influenced by [8], several numerical methods with exponential convergence rates have been developed in the last decade to solve spectral fractional diffusion problems in complex domains. As has been shown in [12], they can all be represented via a rational approximation of $\mathbb{A}^{-\alpha}$. The BURA (best uniform rational approximation) method, originally introduced in [13], also belongs to this group.

Our study is in the spirit of BURA. In [14], a significant improvement in the method was made, as the exponential convergence rate of the new variant is independent of the condition number $\kappa(\mathbb{A})$. Computational complexity estimates of almost optimal behavior of order $O(\log^2 N\, N)$ have been derived, with numerical tests indicating a possible improvement to $O(\log N\, N)$; see, e.g., [15,16] and the references therein. More recently, specialized multilevel iterative methods for the auxiliary linear systems arising in BURA have been presented in [17].

A general principle for BURA methods is that they use the best uniform rational approximation of some scalar function in the interval $[0, 1]$. For more information on the

concept of the methods and some comparative analyses, we recommend the review paper by [15] (see also [16]). A computationally stable numerical solution of the corresponding min–max problem is presented in [18], and the method is implemented in the open access software BRASIL [19].

Preliminary results closest to the topic of this study were presented in [20]. There, the application of the initial version of BURA from [13] to a positive approximation of the inverse of the fractional degree of Stieltjes matrices was discussed. The obtained results can be used, for example, in the case of finite difference approximation of a fractional diffusion problem. In this regard, we note that, in the case of finite element approximation, $\mathbb{A}$ is not a Stieltjes matrix. The provided numerical examples illustrate the behavior of the currently available rational approximation, which is not robust in respect to $\kappa(\mathbb{A})$.

1.3. Our Approach, Contributions and Organization of This Paper

The maximum principle, the discrete maximum principle, and the monotonicity-preserving BURA methods are interrelated qualitative properties. Non-local problems have peculiarities that do not allow for direct generalization of the techniques, developed for standard elliptic equations. In this context, we note the following two specific approaches that are systematically used: (i) elliptic extension problems in $\Omega \times (0, \infty)$ related to fractional problems in $\Omega \subset \mathbb{R}^d$; and (ii) approximation of $\mathbb{A}^{-\alpha}$ by a positive linear combination of the inverses of positive diagonal perturbations of $\mathbb{A}$. In analysis, the approach is not always followed, whereby a qualitative property in the continuous case is preserved using the numerical method.

This paper provides new results on the maximum principle for fractional diffusion–reaction problems. It is proven that the $(2d + 1)$-stencil finite difference method and the linear finite element method satisfy discrete maximum principles. The condition for the finite element mesh is that it does not contain obtuse angles, in which case the stiffness matrix is an M-matrix. However, $\mathbb{A}$ and $\mathbb{A}^{\alpha}$ are not Stieltjes matrices. Sufficient conditions for preserving the non-negativity of BURA solution methods are obtained. These are new results, the starting point of which is the BURA method from [14], which is robust with respect to $\kappa(\mathbb{A})$. Here, we note that qualitatively new difficulties arise in the case when a reactive term is added to the fractional diffusion.

The main contributions of this paper are summarized as follows:

- We develop a unified framework for the maximum principle in both continuous and discrete settings for fractional diffusion–reaction problems, leading to sufficient conditions for discrete maximum principles in finite difference and finite element discretizations. In the FEM case, non-negativity preservation is ensured through the use of lumped mass matrices. The results are documented in Theorem 1 and Remark 1 for the continuous setting and in Lemmas 5 and 6 for the discrete setting, respectively.
- We employ best uniform rational approximation (BURA) techniques for discrete fractional diffusion problems and provide a detailed analysis of monotonicity preservation for rational approximations of fractional operators. Identifying conditions that guarantee non-negativity is essential for obtaining numerically stable and physically meaningful solutions. The results are documented in Theorem 2 and Remark 2.
- Comprehensive numerical experiments validate the theoretical analysis and demonstrate its practical relevance. In particular, comparisons between uniform rational approximation (URA) and BURA methods for discrete fractional diffusion–reaction problems reveal their complementary strengths in terms of accuracy and monotonicity preservation. In Theorem 3, monotonicity preservation for the URA numerical solution method is proven.

- Finally, we propose a hypothesis on the interlacing behavior of BURA elements for fractional diffusion–reaction problems. Although currently unproven, it is strongly supported by numerical evidence and points to promising directions for future research. Experimental results are documented in Table 1 and Figures 1 and 2.

The remainder of the paper is organized as follows: The finite difference method and finite element method discretizations of the spectral fractional diffusion operator are discussed in the next section. The feasibility of lumping the mass matrix is justified. Maximum principles for fractional diffusion and diffusion–reaction problems are proven in Section 3. The main results of this study are presented in the following two sections. Discrete maximum principles for the cases of finite difference and finite element discretizations and monotonicity-preserving BURA methods are analyzed. First, the fractional diffusion problem is addressed in Section 5. Then, the case of fractional diffusion–reactions is studied separately. Perhaps surprisingly to some readers, and unlike the case of a standard elliptic equations, here, the addition of the reactive term led to significant new difficulties. Numerical examples in Section 6 illustrate the obtained theoretical results. Experimental results are also presented, based on which a hypothesis has been formulated, which at this stage has not been proven. Brief concluding remarks are given at the end.

2. Discretization of Fractional Diffusion Operator

We consider the fractional diffusion–reaction problem

$$\begin{aligned} \mathcal{A}^{\alpha} u(x) + q u(x) &= f(x), \qquad x \in \Omega \\ u(x) &= 0, \qquad x \in \partial\Omega, \end{aligned} \tag{4}$$

where $q > 0$ is a constant, $f(x) \in L^2(\Omega)$ is a given source term, and $\mathcal{A}^{\alpha}$ is the fractional diffusion operator defined by (2). In this section, we will briefly discuss some basic properties of matrices arising when discretizing (4) by finite differences on a rectangular grid with N points or an N-dimensional finite element space V_h.

2.1. Finite Difference Discretization

In the case of finite difference discretization, we assume that Ω is a bounded domain with a rectangular polygonal/polytopic boundary $\partial\Omega$. We also assume that diffusion is isotropic, that is, that the coefficient matrix $\mathbf{a}(x)$ is replaced by a scalar positive function $a(x)$. Now let ω_h be a rectangular mesh consistent with $\partial\Omega$. Then the discrete fractional diffusion–reaction problem is described by the linear system

$$(\mathbb{A}^{\alpha} + q\mathbb{I})\mathbf{u} = \mathbf{f}, \tag{5}$$

where $\mathbb{A} \in \mathbb{R}^{N\times N}$ approximates the diffusion operator $\mathcal{A}$, $\mathbf{u}$ is the vector in $\mathbb{R}^N$ of the approximation of $u(x)$ at the interior N grid points of ω_x, and $\mathbf{f} \in \mathbb{R}^N$ denotes the vector of the values of $f(x)$ at the interior grid points.

The simplest two-dimensional example corresponds to $\Omega = (0,1) \times (0,1)$, where ω_h is a $(n+1) \times (n+1)$ square grid with grid size $h = 1/(n+1)$ and $a(x) = 1$. Then, the five-point stencil approximation of the Laplacian gives the matrix $\mathbb{A} \in \mathbb{R}^{N\times N}$, $N = n^2$, which has the following block structure

$$\mathbb{A} = \frac{1}{h^2}\begin{bmatrix} \mathbb{A}_{1,1} & -\mathbb{I} & & & \\ -\mathbb{I} & \mathbb{A}_{2,2} & -\mathbb{I} & & \\ \cdots & \cdots & \cdots & \cdots & \cdots \\ & -\mathbb{I} & \mathbb{A}_{i,i} & -\mathbb{I} & \\ \cdots & \cdots & \cdots & \cdots & \cdots \\ & & & -\mathbb{I} & \mathbb{A}_{n,n} \end{bmatrix}, \quad \mathbb{A}_{i,i} = \begin{bmatrix} 4 & -1 & & \\ -1 & 4 & -1 & \\ \cdots & \cdots & \cdots & \cdots \\ & -1 & 4 & -1 \\ & & -1 & 4 \end{bmatrix}.$$

Here, $\mathbb{A}_{i,i} \in \mathbb{R}^{n\times n}$, $i = 1, \cdots, n$ and $\mathbb{I}$ is the identity matrix in $\mathbb{R}^n$.

In the general case, we consider the finite difference approximation obtained by the balanced method. Then the three-point approximation on $x_{i-1} < x_i < x_{i+1}$ is written in the form

$$-(a(x_i)u'(x_i))' \approx \frac{2}{h_i + h_{i+1}}\left(a_{i+\frac{1}{2}}\frac{u(x_i) - u(x_{i+1})}{h_{i+1}} - a_{i-\frac{1}{2}}\frac{u(x_{i-1}) - u(x_i)}{h_i}\right), \tag{6}$$

where $h_i = x_i - x_{i-1}$, $h_{i+1} = x_{i+1} - x_i$, and $a_{i-\frac{1}{2}} = a(x_i - h_i/2)$ or $a_{i-\frac{1}{2}} = \frac{1}{h_i}\int_{x_{i-1}}^{x_i} a(x)dx$. We apply the same formula in each of the coordinate directions, thus obtaining the $(2d+1)$-point stencil approximation $\mathbb{A}$ of $\mathcal{A}$. We note that, for smoothly varying meshes, the balanced finite difference stencil provides approximately second-order accuracy for the diffusion operator.

A common property of the considered examples of finite difference approximation on a $(2d+1)$-point stencil is that the diffusion matrix $\mathbb{A}$ is symmetric and positive definite. We note in particular that it has in each row/column at most $2d$ nonzero elements, all of which are negative. These properties are of course also valid for the diffusion–reaction matrix $\mathbb{A} + q\mathbb{I}$. In the fractional case, a significant change occurs. The matrix $\mathbb{A}^\alpha + q\mathbb{I}$ is symmetric and positive definite, but dense.

2.2. Finite Element Discretization

Here, Ω is a polygonal/polytopic domain partitioned into triangles/tetrahedra that form the quasi-uniform mesh $\mathcal{T}_h$. We use conforming finite dimensional space $V_h \subset V$ of piece-wise linear functions. Let $\{\phi_j(x)\}_{j=1}^N$ denote the standard nodal basis of V_h. The definition (2) of the fractional power of $\mathcal{A}$ is carried over to the finite-dimensional operator $\mathcal{A}_h$, replacing V with V_h. The finite element approximation $u_h \in V_h$ of $u(x)$ is then given by

$$\mathcal{A}_h^\alpha u_h(x) + q u_h(x) = f_h(x),$$

where $f_h \in V_h$ is defined by the nodal values of $f(x)$. Then the discrete fractional diffusion–reaction problem is described by the linear system

$$(\mathbb{A}^\alpha + q\mathbb{I})\mathbf{u} = \mathbf{f}, \tag{7}$$

where $\mathbf{u}, \mathbf{f} \in \mathbb{R}^N$ are the vectors of the values of $u_h(x)$ and $f(x)$ at the interior nodes of $\mathcal{T}_h$, respectively. Here,

$$\mathbb{A} = \mathbb{M}^{-1}\mathbb{S},$$

where $\mathbb{S}$ and $\mathbb{M}$ are the stiffness and mass matrices; see for more details, e.g., [21]. We note that the matrix $\mathbb{A}$ defined in this way is symmetric and positive definite with respect to the energy scalar product $(\cdot,\cdot)_{\mathbb{M}}$ generated by the mass matrix. Equivalently, $\mathbb{M}^{-1}\mathbb{S}$ is similar to $\mathbb{M}^{-1/2}\mathbb{S}\mathbb{M}^{-1/2}$, which implies that $\mathbb{A}$ is diagonalizable with positive real eigenvalues, thereby justifying the definition of $\mathbb{A}^\alpha$.

The stiffness and mass matrices have a similar structure of nonzero elements. In the case of linear finite elements, the signs of the off-diagonal entries of the stiffness matrix depend on (are controlled by) the angles of the triangles/tetrahedra of the mesh $\mathcal{T}_h$. This does not apply to the mass matrix, which has only non-negative elements.

We also consider a finite element method with a lumped mass matrix $\widetilde{\mathbb{M}}$, defined as follows:

$$(z,w)_\ell = \frac{1}{d+1}\sum_{e\in\mathcal{T}_h}\sum_{i=1}^{d+1}|e|z(V_i)w(V_i) \quad \text{and} \quad \widetilde{\mathbb{M}} = \{(\phi_i,\phi_j)_\ell\}_{i,j}^N.$$

Here, $V_1,\dots,V_{d+1}$ are the vertexes of the d-simplex (triangle or tetrahedral) element e and $|e|$ is its d-dimensional measure. Thus, the alternative discrete fractional diffusion–reaction problem with a lumped mass matrix takes the form

$$(\widetilde{\mathbb{A}}^\alpha + q\mathbb{I})\mathbf{u} = \mathbf{f}, \tag{8}$$

with

$$\widetilde{\mathbb{A}} = \widetilde{\mathbb{M}}^{-1}\mathbb{S}.$$

The lumped mass matrix is diagonal, which on the one hand allows for some reduction in computations. However, the more important goal here is to better preserve non-negativity.

2.3. Assumptions

The assumptions for FDM and FEM discretizations are summarized in the table below. It is important to note that mass lumping is necessary to ensure the discrete maximum principle. Simple one-dimensional counterexamples are well known for unstructured meshes with linear finite elements applied to the standard local equation, e.g.,

$$-u''(x) + u = 1, \quad x \in (0,1), \quad u(0) = u(1) = 0.$$

Property	**FDM**	**FEM**
Domain geometry	Rectangular polygonal/ polyhedral domains	Arbitrary polygonal/ polyhedral domains
Diffusion type	Isotropic	Anisotropic
Mesh	Uniform, structured grid	Unstructured, possibly adaptive
Discretization	$(2d+1)$-point stencil in d dimensions	Linear triangles (2D)/ tetrahedra (3D)
Mass lumping	Not applicable	Standard mass lumping

In this setting, even a coarse mesh with only four interior nodes is sufficient to demonstrate a violation of the discrete maximum principle when the mass matrix is not lumped. Analogous counterexamples can also be constructed for the case of fractional diffusion.

3. Maximum Principle for Fractional Diffusion–Reaction Problems

It is well known that the diffusion–reaction operator $\mathcal{A} + q\mathcal{I}$ satisfies the maximum principle. Owing to the homogeneous boundary conditions, this property is equivalent to non-negativity preservation and monotonicity. More precisely, consider the equation $\mathcal{A}u(x) + qu(x) = f(x)$. If $f(x) \geq 0$, then the corresponding solution satisfies $u(x) \geq 0$. Moreover, if $f_1(x) \geq f_2(x)$, then the associated solutions satisfy $u_1(x) \geq u_2(x)$. Consequently, under homogeneous boundary conditions, these three notions may be used interchangeably. The corresponding definitions extend naturally to the discrete case. In this

section, we will prove that a similar property is also valid in the case of fractional diffusion; see Equation (4).

Lemma 1. *The solution of fractional diffusion–reaction problem is obtained from the relation* $u(x) = \mathcal{U}(x,0)$ *where* $\mathcal{U} : \Omega \times \mathbb{R}_+ \to \mathbb{R}$ *is a solution of the equation*

$$-div\Big(y^{1-2\alpha}\mathbf{A}(x)\nabla\mathcal{U}(x,y)\Big) = 0, \quad (x,y) \in \mathcal{C} := \Omega \times \mathbb{R}_+. \tag{9}$$

Here, as well as later in the article, $\mathbf{A}(x) = diag(\mathbf{a}(x),1)$, $\mathcal{U}(\cdot,y)$ *satisfies the homogeneous boundary conditions in* (4)*, and, in addition,*

$$\lim_{y\to\infty}\mathcal{U}(x,y) = 0 \ \text{ as well as } \ \lim_{y\to 0^+}\Big(-y^{1-2\alpha}\,\mathcal{U}_y(x,y) + d_\alpha q\,\mathcal{U}(x,y)\Big) = d_\alpha f(x), \quad x \in \Omega, \tag{10}$$

where

$$d_\alpha = 2^{1-2\alpha}\frac{\Gamma(1-\alpha)}{\Gamma(\alpha)} > 0$$

is a dimension-independent constant involving the gamma function.

Proof. The boundary condition (10) is analogous to the corresponding condition in [22], where a parabolic fractional diffusion equation is considered. The only modification consists in replacing the time derivative by the reaction term. With this observation, the proof of the lemma follows by repeating the arguments of ([22], Section 2.4), and we may therefore utilise the solution representation described below. We recall that $\{\lambda_i, \psi_i(x)\}$ are the eigenpairs of the operator $\mathcal{A}$ (see (2)). If

$$u(x) = \sum_{i=1}^{\infty} u_k\psi_k(x)$$

solves (4), then its extension is given by

$$\mathcal{U}(x,y) = \sum_{i=1}^{\infty} u_k\psi_k(x)\zeta_k(y),$$

where each function $\zeta_k(y)$ satisfies

$$\zeta_k''(y) + (1-2\alpha)y^{-1}\zeta_k'(y) = \lambda_k\zeta_k(y), \quad \zeta_k(0) = 1, \quad \lim_{y\to\infty}\zeta_k(y) = 0.$$

□

The variational formulation of the Equations (9) and (10) is posed in the weighted Sobolev space

$$\widetilde{V} := \{\mathcal{V} \in H^1_{\mathcal{C},y^\alpha} : \mathcal{V}(x,y) = 0 \text{ if } x \in \partial\Omega\},$$

where

$$H^1_{\mathcal{C},y^\alpha} = \{w : \int_{\mathcal{C}} y^{1-2\alpha}(|\nabla w|^2 + w^2)dxdy < \infty\}.$$

Then the weak formulation of (9) reads as follows: find $\mathcal{U} \in \widetilde{V}$ such that

$$\int_{\mathcal{C}} y^{1-2\alpha}\mathbf{A}\nabla\mathcal{U}(x,y)\cdot\nabla\mathcal{V}(x,y)d(x,y) + \int_\Omega d_\alpha q\,\mathcal{U}(x,0)\mathcal{V}(x,0)dx = \int_\Omega d_\alpha f(x)\mathcal{V}(x,0)dx \quad \forall\,\mathcal{V} \in \widetilde{V}. \tag{11}$$

Theorem 1. *Assume that* $1/2 < \alpha < 1$ *and* $f(x) \geq 0$ *in* Ω*. Then* $u(x) = \mathcal{U}(x,0) \geq 0$ *in* Ω*, i.e., the fractional diffusion–reaction problem satisfies the maximum principle.*

Proof. To proceed, we truncate the infinite interval $\mathbb{R}_+$ to $(0, L)$, where $L > 0$, and introduce the auxiliary space $\widetilde{V}_L := \{\mathcal{V}_L \in H^1_{\Omega\times(0,L)} : \mathcal{V}_L(x,y) = 0 \text{ if } x \in \partial\Omega \text{ and } \mathcal{V}_L(x,L) = 0, x \in \Omega\}$. Then, the equation corresponding to (11) takes the following form: find $\mathcal{U}_L \in \widetilde{V}_L$ such that

$$\int_{\Omega\times(0,L)} y^{1-2\alpha}\mathbf{A}\nabla\mathcal{U}_L(x,y)\cdot\nabla\mathcal{V}_L(x,y)d(x,y) + \int_\Omega d_\alpha q\mathcal{U}_L(x,0)\mathcal{V}_L(x,0)dx = \int_\Omega d_\alpha f(x)\mathcal{V}_L(x,0)dx \quad \forall\, \mathcal{V}_L \in \widetilde{V}_L. \tag{12}$$

We now consider the one-dimensional selfadjoint positive definite eigenvalue problem: find $\{\nu_L, \vartheta_L(y)\}$, $\vartheta_L \in \dot{H}^1_{(0,L)}$, such that

$$\int_0^L y_L^{1-2\alpha}\vartheta_L'(y)v_L'(y)dy = \nu_L\int_0^L y_L^{1-2\alpha}\vartheta_L(y)v_L(y)dy \quad \forall v_L \in \dot{H}^1_{(0,L)}. \tag{13}$$

Here, $\dot{H}^1_{(0,L)} := \{v_L \in H^1_{(0,L)} : v_L(L) = 0\}$. The eigenvalues of (13) are real and positive, and we assume that the eigenfunctions $\{\vartheta_{L,k}(y)\}_{k=1}^\infty$ are normalised, i.e.,

$$\int_0^L y^{1-2\alpha}\vartheta_{L,i}(y)\vartheta_{L,j}(y)dy = \delta_{ij},$$

where δ_{ij} is the Kronecker symbol.

Now, we apply a spectral decomposition of (12) over the extended variable $y \in (0, L)$. We recall that, in the discrete case of fractional Laplacian, diagonalization based on such a spectral decomposition was introduced in [22]. Thus, the solution of the $d+1$ dimensional truncated problem is expressed by the solutions of a series of d dimensional problems in Ω. In this way, we get the representation

$$\mathcal{U}_L(x,y) = \sum_{i=1}^\infty \vartheta_{L,i}^2(y)[\mathcal{A} + (d_\alpha q + \nu_i)\mathcal{I}]^{-1}d_\alpha f(x)$$

and, therefore,

$$u_L(x) = \sum_{i=1}^\infty \vartheta_{L,i}^2(0)[\mathcal{A} + (d_\alpha q + \nu_{L,i})\mathcal{I}]^{-1}d_\alpha f(x). \tag{14}$$

Since the standard (local) diffusion–reaction equation satisfies the maximum principle, i.e., preservers monotonicity, $[\mathcal{A} + (d_\alpha q + \nu_{L,i})\mathcal{I}]^{-1}d_\alpha f(x) \geq 0$, and therefore $u_L(x) \geq 0$.

We now exploit the exponential decay of $\mathcal{U}(x,y)$ as $y \to \infty$, which implies the convergence of $\mathcal{U}_L(x,y)$ to $\mathcal{U}(x,y)$ in a Sobolev space of order α; see, for example, [22,23] . Consequently,

$$\lim_{L\to\infty} ||\mathcal{U}_x - \mathcal{U}_{x,L}||_{H^\alpha(0,\infty)} = 0.$$

Here, $\mathcal{U}_x(y) := \mathcal{U}(x,y)$, for $y \in (0,\infty)$, while $\mathcal{U}_{x,L}(y) := \mathcal{U}_L(x,y)$ for $y \in (0,L)$ and $\mathcal{U}_{x,L}(y) := 0$ for $y \in [L,\infty)$. Therefore,

$$\lim_{L\to\infty}(\mathcal{U}_x - \mathcal{U}_{x,L}) = 0.$$

We note that the final consequence holds if and only if $\alpha > 0.5$, which follows from the one-dimensional Sobolev embedding theorem, where the L^∞ norm is controlled by the H^α norm. Consequently,

$$\lim_{L\to\infty} ||u - u_l||_{L^\infty(0,\infty)} = 0$$

with rate e^{-L}. Hence,

$$u(x) = \lim_{L\to\infty} u_L(x) \geq 0,$$

which completes the proof of the theorem. □

https://doi.org/10.3390/sym18020272

Remark 1. *It should be noted that the restriction $\alpha > 1/2$ stems from the method of proof employed in Theorem 1 and may therefore be viewed as a limitation of the argument rather than a definitive threshold. To the best of our knowledge, no counterexamples to the maximum principle are currently known for $\alpha \leq 1/2$. While heuristic considerations suggest that the scope of Theorem 1 might extend to $\alpha \in (0,1)$, a rigorous justification of this conjecture is presently unavailable and remains an open problem.*

4. Discrete Fractional Diffusion Problems

4.1. Discrete Maximum Principle: Finite Difference Case

For standard (local) elliptic boundary value problems, Stieltjes matrices are the most often used tool to prove the discrete maximum principle. This is the class of real symmetric positive definite matrices with non-positive off-diagonal elements. In other words, these are symmetric M-matrices. We recall that the inverse of every Stieltjes matrix is elementwise non-negative.

Here and further in the article, we assume that the finite difference approximation is defined on the $(2d+1)$-point stencil. Thus, $\mathbb{A}$ is a Stieltjes matrix.

Sufficient conditions for functions which preserve the class of Stieltjes matrices are studied in [3]. As a conclusion from the main theorem, three examples of nontrivial functions which map Stieltjes matrices into Stieltjes matrices are presented. The first of them is $\mathbb{A}^\alpha$ for $\alpha \in (0,1)$. Therefore, the following lemma holds:

Lemma 2. *Let Ω be a bounded domain with a rectangular polygonal/polytopic boundary $\partial\Omega$ and ω_h be a rectangular mesh consistent with $\partial\Omega$. We assume also that the finite difference approximation is obtained by balanced method applying (6) in each of the coordinate directions. Then the discrete fractional diffusion problem*

$$\mathbb{A}^\alpha \mathbf{u} = \mathbf{f}$$

satisfies the maximum principle and if $f(x) \geq 0$ in Ω (i.e., $\mathbf{f} \geq 0$), then $\mathbf{u} \geq 0$.

4.2. Discrete Maximum Principle: Finite Element Case

We consider discretization by linear finite elements defined on the mesh $\mathcal{T}_h$, which partitions Ω into triangles/tetrahedra. When analysing the finite element case, here and further in the paper we assume that there are no obtuse $e \in \mathcal{T}_h$. Under such a condition, the stiffness matrix $\mathbb{S}$ is a Stieltjes matrix. This property follows from the representation of the element stiffness matrices in explicit form for both triangles and tetrahedra, where, up to a scaling constant, all off-diagonal elements are cotangents of the corresponding angles.

The mass matrix is positive regardless of the mesh $e \in \mathcal{T}_h$, thus preserving the sign of the right-hand side of the discrete problem. However, this is not enough to guarantee the discrete maximum principle. This is the reason why we consider a finite element approximation with a lumped mass matrix $\widetilde{\mathbb{M}}$, as already defined in the previous section. Then the discrete fractional diffusion problem is written in the form $\widetilde{\mathbb{A}}^\alpha \mathbf{u} = \widetilde{\mathbb{M}}\mathbf{f}$,$\widetilde{\mathbb{A}} = \widetilde{\mathbb{M}}^{-1}\mathbb{S}$.

Although it has only non-positive off-diagonal elements, $\widetilde{\mathbb{A}}$ is not a Stieltjes matrix. This is particularly due to the fact that the matrix is not symmetric. Regardless of the former, the following lemma holds:

Lemma 3. *Let Ω be a bounded domain with a polygonal/polytopic boundary $\partial\Omega$, and let $\mathcal{T}_h$ be a mesh of non-obtuse triangles/tetrahedra that is compatible with $\partial\Omega$. We also assume that finite element discretization with a lumped mass matrix is applied. Then the discrete fractional diffusion problem*

$$\widetilde{\mathbb{A}}^\alpha \mathbf{u} = \mathbf{f},$$

satisfies the maximum principle and if $f(x) \geq 0$ *in* Ω, *then* $\mathbf{u} \geq 0$.

At the end of the next section, we will show how the proof of the lemma follows from the properties of the best uniformly rational approximation of $\widetilde{\mathbb{A}}^{-\alpha}$.

4.3. Monotonicity-Preserving BURA Numerical Solution

Here, we apply the rescaled BURA as presented in [14]. First, some basic properties of the method are presented. Let us consider the set of rational functions

$$\mathcal{R}_k = \{r_k(z) := P_k(z)/Q_k(z), P_k \in \mathcal{P}_k, \text{ and } Q_k \in \mathcal{P}_k\},$$

where $\mathcal{P}_k$ is the set of algebraic polynomials of degree k with real coefficients. The best uniform rational approximation (BURA) $r_{\alpha,k}(z)$ of z^α on $[0,1]$ is then defined as

$$r_{\alpha,k}(z) := \min_{r_k(z)\in\mathcal{R}_k} \max_{z\in[0,1]} |r_k(z) - z^\alpha|.$$

Then the BURA approximation of the solution of fractional diffusion system is given by

$$\mathbf{u} \approx \mathbf{u}_k = \mu_1^{-\alpha} r_{\alpha,k}(\mu_1 \mathbb{A}^{-1})\mathbf{f}$$

where $\mu_1 > 0$ is the first eigenvalue of $\mathbb{A}$. The roots ζ_i and poles d_i of $r_{\alpha,k}(z)$ satisfy the interlacing inequalities (see, e.g., [24]):

$$0 > \zeta_1 > d_1 > \zeta_2 > d_2 > \cdots > \zeta_k > d_k. \tag{15}$$

Lemma 4. *Let* $P_k(z)$ *and* $Q_k(z)$ *be polynomials of degree* k *with real coefficients. Suppose that the roots* $\{\zeta_i\}_1^k$ *and* $\{d_i\}_1^k$ *of* P_k *and* Q_k, *respectively, satisfy the interlacing property*

$$0 > \zeta_1 > d_1 > \zeta_2 > d_2 > \cdots > \zeta_k > d_k.$$

Let $r_k(z) = P_k(z)/Q_k(z)$ *and* $r_k(1) > 0$. *Then*

(i) $r_k(z) = c_0 + \sum_{i=1}^k \frac{c_i}{z-d_i}$, $\quad c_0 > 0;\ c_i < 0,\ i = 1,\ldots,k;$

(ii) $r_k(\mu z^{-1}) = \tilde{c}_0 + \sum_{i=1}^k \frac{\tilde{c}_i}{z-\tilde{d}_i}$, $\quad \mu > 0;\quad \tilde{c}_i > 0,\ i = 0,\ldots,k;\ \tilde{d}_i < 0,\ i = 1,\ldots,k.$

Proof. The claim is similar to Proposition 2.1 in [14], but, for the sake of completeness, we will provide a slightly different proof here, as well. Denote by $\operatorname{sgn}(x)$ the sign of the real number x and extend the definition also for $\pm\infty$, i.e., $\operatorname{sgn}(\pm\infty) = \pm 1$. Further, denote by $r_k(d^+)$ the right-hand limit of $r_k(z)$ at d, respectively, by $r_k(d^-)$ the left-hand limit of $r_k(z)$ at d.

Since all roots of $Q_k(z)$ are real and simple, and the degree of $P_k(z)$ is equal to the degree of $Q_k(z)$, we know that partial fraction decompositions of the types (i) and (ii) exist. Thus, we just need to compute the signs of the coefficients. Due to the interlacing property, we have that $\operatorname{sgn}(r_k(z))$ is constant in the interval $(\zeta_1, +\infty)$. But $r_k(1) > 0$ and $1 \in (\zeta_1, +\infty)$; thus, the sign function is one on the above interval. Now, in the interval $(d_1, +\infty)$, there is only one zero of $P_k(z)$ and no zeros of $Q_k(z)$, which gives rise to

$$\operatorname{sgn}\big(r_k(d_1^+)\big) \cdot \operatorname{sgn}(r_k(1)) = -1 \qquad \Longrightarrow \qquad r_k(d_1^+) = -\infty.$$

The latter implies $\operatorname{sgn}(c_1) = -1$. Repeating the above procedure, we get

$$\operatorname{sgn}\big(r_k(d_1^-)\big) \cdot \operatorname{sgn}\big(r_k(d_1^+)\big) = -1 \ \&\ \operatorname{sgn}\big(r_k(d_1^-)\big) \cdot \operatorname{sgn}\big(r_k(d_2^+)\big) = -1 \qquad \Longrightarrow \qquad r_k(d_2^+) = -\infty,$$

and $\operatorname{sgn}(c_2) = -1$. By induction, we conclude that $\operatorname{sgn}(c_i) = -1$ for all $i = 1, 2, \ldots, k$. Finally, $r_k'(z) = \sum_{i=1}^{k} -c_i/(z-d_i)^2$ is strictly positive when $z \in (d_1, +\infty)$. Therefore,

$$c_0 = \lim_{z \to +\infty} r_k(z) > r_k(1) > 0.$$

For (ii), direct computations lead to

$$r_k(\mu z^{-1}) = c_0 + \sum_{i=1}^{k} \frac{c_i}{\mu z^{-1} - d_i} = \left(c_0 - \sum_{i=1}^{k} \frac{c_i}{d_i} \right) + \sum_{i=1}^{k} \frac{-\mu c_i/d_i^2}{z - \mu/d_i}.$$

Thus $\tilde{c}_0 = c_0 - \sum_{i=1}^{k} c_i/d_i = r_k(0) > 0$, due to $0 \in (\zeta_1, +\infty)$, $\tilde{c}_i = -\mu c_i/d_i^2 > 0$, and $\tilde{d}_i = \mu/d_i < 0$ for all $i = 1, \ldots, k$. The proof is completed. □

Since $|r_{\alpha,k}(1) - 1| = E_{\alpha,k} \ll 1$, where $E_{\alpha,k}$ is the BURA error, (15), together with Lemma 4(ii), ensures that the BURA approximation of $\mathbb{A}^{-\alpha}\mathbf{f}$ can be written in the form

$$\mathbf{u} \approx \mathbf{u}_k = \tilde{c}_0 \mathbf{f} + \sum_{i=1}^{k} \tilde{c}_i (\mathbb{A} - \tilde{d}_i \mathbb{I})^{-1} \mathbf{f} := \sum_{i=0}^{k} \mathbf{u}_k^{(i)}, \tag{16}$$

where $\tilde{c}_0 > 0$, and $\tilde{c}_i > 0$, $\tilde{d}_i < 0$ for $1 \le i \le k$.

In the case of finite difference discretization and under the assumptions already made, $\mathbb{A} - \tilde{d}_i \mathbb{I}$ is a Stieltjes matrix. Therefore, if $f(x) \ge 0$ in Ω, i.e., $\mathbf{f} \ge 0$, then $\mathbf{u}_k^{(i)} \ge 0$. In other words, the BURA method preserves monotonicity.

The situation changes when discretizing by the finite element method, where the matrix $\widetilde{\mathbb{A}} = \widetilde{\mathbb{M}}^{-1}\mathbb{S}$ is not Stieltjes. In this case, however, we can rewrite (16) as follows:

$$\mathbf{u} \approx \mathbf{u}_k = \tilde{c}_0 \mathbf{f} + \sum_{i=1}^{k} \tilde{c}_i (\widetilde{\mathbb{M}}^{-1}\mathbb{S} - \tilde{d}_i \mathbb{I})^{-1} \mathbf{f} = \tilde{c}_0 \mathbf{f} + \sum_{i=1}^{k} \tilde{c}_i (\mathbb{S} - \tilde{d}_i \widetilde{\mathbb{M}})^{-1} \widetilde{\mathbb{M}} \mathbf{f} := \sum_{i=0}^{k} \mathbf{u}_k^{(i)}. \tag{17}$$

Here, $\mathbb{S} - \tilde{d}_i \widetilde{\mathbb{M}}$ is a Stieltjes matrix and, therefore, if $f(x) \ge 0$ in Ω, i.e., $\mathbf{f} \ge 0$ and $\widetilde{\mathbb{M}}\mathbf{f} \ge 0$, then $\mathbf{u}_k^{(i)} \ge 0$, and again the BURA method preserves monotonicity.

We summarize the results, and thus we obtain the following theorem:

Theorem 2. *Let the fractional diffusion problem be discretized using the finite difference method or the finite element method, whereby the conditions of Lemma 2 or Lemma 3 are satisfied, respectively. Then the BURA numerical solution method, defined by* (16) *or* (17)*, preserves the monotonicity of the corresponding fractional diffusion linear system.*

Remark 2. *As shown in [14], the BURA numerical solution of fractional diffusion system (exponentially) converges to the exact solution, i.e.,* $\lim_{k\to\infty} \mathbf{u}_k = \mathbf{u}$. *Therefore, if the assumptions regarding the finite element method discretization in Lemma 3 are satisfied, and if* $f(x) \ge 0$*, then* $\mathbf{u}_k \ge 0$*, hence* $\mathbf{u} \ge 0$.

5. Discrete Fractional Diffusion–Reaction Problems

5.1. Discrete Maximum Principle: Finite Difference Case

The result in the finite difference case follows directly from the arguments in Section 4.1. We recall that the approximation is defined on the $(2d+1)$-point stencil; then $\mathbb{A}$ is a Stieltjes matrix and, consequently, $\mathbb{A}^{\alpha}$ is a Stieltjes matrix.

From the definition, it is clear that the sum of two Stieltjes matrices is another Stieltjes matrix. The same applies in particular if consider a positive diagonal shift. Therefore, the

finite difference diffusion–reaction matrix $\mathbb{A}^{\alpha} + q\mathbb{I}$ is a Stieltjes matrix. Thus we obtain that the following lemma holds:

Lemma 5. *Let Ω be a bounded domain with a rectangular polygonal/polytopic boundary $\partial\Omega$ and ω_h be a rectangular mesh consistent with $\partial\Omega$. We assume also that the finite difference approximation is obtained by balanced method applying (6) in each of the coordinate directions. Then the discrete fractional diffusion–reaction problem*

$$(\mathbb{A}^{\alpha} + q\mathbb{I})\mathbf{u} = \mathbf{f}$$

satisfies the maximum principle and if $f(x) \geq 0$ in Ω (i.e., $\mathbf{f} \geq 0$), then $\mathbf{u} \geq 0$.

5.2. Discrete Maximum Principle: Finite Element Case

Here, we strictly adhere to the finite element discretization framework from Section 4.2. However, to prove the maximum principle, we will need an alternative approach.

Lemma 6. *Let Ω be a bounded domain with a polygonal/polytopic boundary $\partial\Omega$, and let $\mathcal{T}_h$ be a mesh of non-obtuse triangles/tetrahedra that is compatible with $\partial\Omega$. We also assume that finite element discretization with a lumped mass matrix is applied. Then the discrete fractional diffusion–reaction problem*

$$\left(\widetilde{\mathbb{A}}^{\alpha} + q\mathbb{I}\right)\mathbf{u} = \mathbf{f},$$

satisfies the maximum principle and if $f(x) \geq 0$ in Ω, then $\mathbf{u} \geq 0$.

Proof. Let us consider the elliptic extension problem introduced in Lemma 1, and let us replace $V \subset H^1(\Omega)$ with the finite element space of piecewise linear functions $V_h \subset V$ corresponding to $\mathcal{T}_h$. Then, the finite element approximation of the solution of the fractional diffusion–reaction problem is obtained from the discrete representation of (14), i.e.,

$$\mathcal{U}_h(x,y) = \sum_{i=1}^{\infty} \vartheta_i^2(y)[\mathcal{A}_h + d_{\alpha}q + \nu_i)\mathcal{I}]^{-1} d_{\alpha} f_h(x)$$

and

$$u_h(x) = \sum_{i=1}^{\infty} \vartheta_i^2(0)[\mathcal{A}_h + (d_{\alpha}q + \nu_i)\mathcal{I}]^{-1} d_{\alpha} f_h(x). \tag{18}$$

Thus, in the case of finite element discretization with a lumped mass matrix, from (18) we obtain

$$\mathbf{u} = \sum_{i=1}^{\infty} \vartheta_i^2(0)[\widetilde{\mathbb{A}} + (d_{\alpha}q + \nu_i)\mathbb{I}]^{-1} d_{\alpha}\mathbf{f} = \sum_{i=1}^{\infty} \vartheta_i^2(0)\left[\mathbb{S} + (d_{\alpha}q + \nu_i)\widetilde{\mathbb{M}}\right]^{-1} d_{\alpha}\widetilde{\mathbb{M}}\mathbf{f} \geq 0, \tag{19}$$

which completes the proof. We note that in the last inequality we used that $\mathbb{S} + (d_{\alpha}q + \nu_i)\widetilde{\mathbb{M}}$ is a Stieltjes matrix, which is not true if the mass matrix is not lumped. □

5.3. Monotonicity-Preserving URA and BURA Numerical Solution

Let us write Formula (19) in the form

$$\mathbf{u} = R_q(\widetilde{\mathbb{A}})\mathbf{f}$$

where

$$R_q(t) = \sum_{i=1}^{\infty} \frac{\vartheta_i^2(0)}{t + d_{\alpha}q + \nu_i}, \qquad t \in [\mu_1, \infty).$$

Then, when the infinite sum is truncated, e.g., keeping the first k terms, we will obtain a rational approximation of $\mathbf{u}$ of degree k. It is easy to see that such a rational approximation

preserves monotonicity. However, it is not so easy to find the coefficients ϑ_i and ν_i. Such a rational approximation may also not be the best. This is the reason why methods based on uniform rational approximation are preferred here.

We will now consider the URA and BURA methods introduced in [21] for numerically solving the fractional diffusion–reaction system $[\widetilde{\mathbb{A}}^{\alpha} + q\mathbb{I}]\mathbf{u} = \mathbf{f}$. They are based on the two rational approximations of

$$g(z) = \frac{1}{z^{-\alpha} + q} = \frac{z^{\alpha}}{1 + qz^{\alpha}}$$

on $z \in [0, 1]$. We first introduce

$$\bar{r}_{\alpha,q,k}(z) := \frac{r_{\alpha,k}(z)}{1 + qr_{\alpha,k}(z)},$$

where $r_{\alpha,k}(z)$ is the best uniformly rational approximation of z^{α}, which we analyzed in Section 4.3. Second, we introduce the best uniformly rational approximation $r_{\alpha,q,k}(z) \in \mathcal{R}_k$. Then, the following two approximations of $\mathbf{u} = [\widetilde{\mathbb{A}}^{\alpha} + q\mathbb{I}]^{-1}\mathbf{f}$ were proposed, thus defining the following two alternative numerical methods:

(a) *URA method:* $\mathbf{u}_k^{(1)} := \bar{r}_{\alpha,q,k}(\widetilde{\mathbb{A}}^{-1})\mathbf{f}$ & (b) *BURA method:* $\mathbf{u}_k^{(2)} := r_{\alpha,q,k}(\widetilde{\mathbb{A}}^{-1})\mathbf{f}$.

We stress that the BURA method uses the best uniform rational approximation, while URA is based on an otherwise constructed rational approximation. Specifically, the URA is obtained by the best uniform rational approximation of the z^{α} terms in the right-hand representation of $g(x)$. For a given $q > 0$, both methods have an exponential rate of convergence with respect to k. However, as might be expected, error estimates show the better accuracy of BURA, which is also confirmed by the numerical tests conducted.

From a theoretical point of view, one of the advantages of the URA method is that the corresponding roots and poles satisfy interlacing inequalities similar to (15) (see [21]). Therefore, the analogues of the representations (16) and (17) are valid, which, in conclusion, leads to the following theorem:

Theorem 3. *Let the fractional diffusion–reaction problem be discretized using the finite difference method or the finite element method, whereby the conditions of Lemma 2 or Lemma 3 are satisfied, respectively. Then the URA numerical solution method preserves the monotonicity of the corresponding fractional diffusion–reaction linear system.*

The validity of interlacing inequalities for roots and poles but without theoretical proof has also been experimentally observed for the BURA method. This issue will be discussed in the next section. If we assume that such a property holds, from Lemma 4, we immediately obtain that the BURA numerical solution method for fractional diffusion–reaction systems also preserves monotonicity.

6. Numerical Examples

In this section, we demonstrate the monotonicity preservation of the URA solution method for fractional diffusion–reaction systems, and we also provide numerical evidence that the corresponding BURA solution method also preserves monotonicity. Thus, the experimental study has two primary objectives: first, to validate the theoretical results, and second, to illustrate phenomena that extend beyond the current theory. The latter objective specifically concerns the case $\alpha = 0.5$, noting that the rigorous analysis based on Theorem 1 applies to the sub-diffusive regime with strictly $\alpha \in (0.5, 1)$.

6.1. The Interlacing Property for Roots and Poles of BURA Elements

Using the BRASIL software [19], we have computed the zeros and poles of all BURA elements $r_{\alpha,q,k}(z)$ and all URA elements $\bar{r}_{\alpha,q,k}(z)$ for all choices of $\alpha \in \{0.25, 0.50, 0.75\}$, $q \in \{1, 2, 4, 8, 16, 32, 100, 200, 400\}$, and $1 \leq k \leq 10$. For each one of the 270 computed BURA elements, the interlacing property (15) holds true. Four particular examples ($\alpha \in \{0.50, 0.75\}$, $q \in \{1, 100\}$, $k = 6$), together with their URA counterparts, are documented in Table 1.

Table 1. An illustration of the interlacing property for the BURA and URA elements.

	Zeros/Poles	$i = 1$	$i = 2$	$i = 3$	$i = 4$	$i = 5$	$i = 6$
$r_{0.5,1,6}(z)$	$\{\widetilde{\zeta}_i\}_{i=1}^6$	-5.27×10^{-8}	-1.14×10^{-5}	-3.30×10^{-4}	-4.94×10^{-3}	-5.41×10^{-2}	-6.10×10^{-1}
	$\{\widetilde{d}_i\}_{i=1}^6$	-1.26×10^{-6}	-6.83×10^{-5}	-1.31×10^{-3}	-1.52×10^{-2}	-1.34×10^{-1}	-1.21×10^{0}
$\bar{r}_{0.5,1,6}(z)$	$\{\bar{\zeta}_i\}_{i=1}^6$	-8.14×10^{-8}	-1.75×10^{-5}	-5.02×10^{-4}	-7.28×10^{-3}	-7.47×10^{-2}	-7.72×10^{-1}
	$\{\bar{d}_i\}_{i=1}^6$	-1.95×10^{-6}	-1.05×10^{-4}	-1.95×10^{-3}	-2.15×10^{-2}	-1.73×10^{-1}	-1.45×10^{0}
$r_{0.75,1,6}(z)$	$\{\widetilde{\zeta}_i\}_{i=1}^6$	-3.70×10^{-7}	-6.84×10^{-5}	-1.29×10^{-3}	-1.28×10^{-2}	-9.67×10^{-2}	-7.82×10^{-1}
	$\{\widetilde{d}_i\}_{i=1}^6$	-2.69×10^{-5}	-6.69×10^{-4}	-7.39×10^{-3}	-5.59×10^{-2}	-3.33×10^{-1}	-1.53×10^{0}
$\bar{r}_{0.75,1,6}(z)$	$\{\bar{\zeta}_i\}_{i=1}^6$	-4.84×10^{-7}	-8.95×10^{-5}	-1.68×10^{-3}	-1.65×10^{-2}	-1.20×10^{-1}	-9.27×10^{-1}
	$\{\bar{d}_i\}_{i=1}^6$	-3.52×10^{-5}	-8.73×10^{-4}	-9.51×10^{-3}	-6.94×10^{-2}	-3.86×10^{-1}	-1.68×10^{0}
$r_{0.5,100,6}(z)$	$\{\widetilde{\zeta}_i\}_{i=1}^6$	-6.05×10^{-10}	-1.36×10^{-7}	-4.38×10^{-6}	-8.61×10^{-5}	-1.66×10^{-3}	-4.99×10^{-2}
	$\{\widetilde{d}_i\}_{i=1}^6$	-1.44×10^{-8}	-7.75×10^{-7}	-1.42×10^{-5}	-1.60×10^{-4}	-2.06×10^{-3}	-5.27×10^{-2}
$\bar{r}_{0.5,100,6}(z)$	$\{\bar{\zeta}_i\}_{i=1}^6$	-8.14×10^{-8}	-1.75×10^{-5}	-5.02×10^{-4}	-7.28×10^{-3}	-7.47×10^{-2}	-7.72×10^{-1}
	$\{\bar{d}_i\}_{i=1}^6$	-1.59×10^{-6}	-5.32×10^{-5}	-7.00×10^{-4}	-7.95×10^{-3}	-7.66×10^{-2}	-7.80×10^{-1}
$r_{0.75,100,6}(z)$	$\{\widetilde{\zeta}_i\}_{i=1}^6$	-2.44×10^{-8}	-4.57×10^{-6}	-9.05×10^{-5}	-1.04×10^{-3}	-1.09×10^{-2}	-1.50×10^{-1}
	$\{\widetilde{d}_i\}_{i=1}^6$	-1.78×10^{-6}	-4.47×10^{-5}	-4.68×10^{-4}	-2.35×10^{-3}	-1.29×10^{-2}	-1.54×10^{-1}
$\bar{r}_{0.75,100,6}(z)$	$\{\bar{\zeta}_i\}_{i=1}^6$	-4.84×10^{-7}	-8.95×10^{-5}	-1.68×10^{-3}	-1.65×10^{-2}	-1.20×10^{-1}	-9.327×10^{-1}
	$\{\bar{d}_i\}_{i=1}^6$	-3.38×10^{-5}	-6.32×10^{-4}	-3.21×10^{-3}	-1.83×10^{-2}	-1.23×10^{-1}	-9.33×10^{-1}

Let us recall that, by $\{\zeta_i\}_1^k$ and $\{d_i\}_1^k$, we denoted the zeros and poles of $r_{\alpha,k}$, respectively. Analogously, we denoted, by $\{\bar{\zeta}_i\}_1^k$ and $\{\bar{d}_i\}_1^k$, the zeros and poles of the URA element $\bar{r}_{\alpha,q,k}$. In [21], it was proven that

$$0 > \bar{\zeta}_1 = \zeta_1 > \bar{d}_1 > d_1 > \bar{\zeta}_2 = \zeta_2 > \bar{d}_2 > d_2 > \cdots > \bar{\zeta}_k = \zeta_k > \bar{d}_k > d_k > -\infty, \tag{20}$$

which is numerically validated in Table 1. Similarly, if we denote by $\{\widetilde{\zeta}_i\}_1^k$ and $\{\widetilde{d}_i\}_1^k$ the zeros and poles of the BURA element $r_{\alpha,q,k}$, all the numerical experiments satisfy the interlacing property

$$0 > \widetilde{\zeta}_1 > \zeta_1 > \widetilde{d}_1 > \bar{d}_1 > d_1 > \widetilde{\zeta}_2 > \zeta_2 > \widetilde{d}_2 > \bar{d}_2 > d_2 > \cdots > \widetilde{\zeta}_k > \zeta_k > \widetilde{d}_k > \bar{d}_k > d_k > -\infty. \tag{21}$$

Furthermore, we observe that, for fixed α and k, the distances $\bar{\zeta}_i - \bar{d}_i$ and $\widetilde{\zeta}_i - \widetilde{d}_i$ monotonically decrease when q monotonically increases. For example, when $\alpha = 0.75$, $q = 100$, $k = 6$, we have $\bar{\zeta}_6 - \bar{d}_6 \approx 3 \cdot 10^{-3}$ and $\widetilde{\zeta}_6 - \widetilde{d}_6 \approx 4 \cdot 10^{-3}$.

6.2. Monotonicity Preservation

We demonstrate the monotonicity preservation of the BURA/URA solution methods for fractional Laplacian reaction systems on a couple of 2D examples. For detailed explanation of the experimental setup and the derivation of the presented results, please see Appendix A. A uniform rectangular mesh with $h = 2^{-10}$ is introduced in $\Omega = [0,1] \times [0,1]$. Consequently, the size of the discrete problem (i.e., the number of unknowns) is $N = (2^{10} - 1) \times (2^{10} - 1) = 1046529$. In this formulation of the problem, finite difference discretization on a five-point stencil and linear finite element discretization

with a lumped mass matrix are equivalent. Both considered variants of the right-hand-side $f(x)$ are piecewise constant functions. Such examples are representative due to the Runge's phenomenon, i.e., the inability of nonlinear interpolatory polynomials to preserve monotonicity on such data.

The first choice $f(x) = f_1(x)$ consists of the constant one, apart from the patch $[1/4, 1/2] \times [1/4, 1/2]$, where the function is zero. In the second case, $f(x) = f_2(x)$ is a 4×4 chessboard-type of function, where the values $0, 1$ alternate (see Figure 1). In both cases, the solution is characterized by boundary and interface layers whose steepness decreases with increasing α or q.

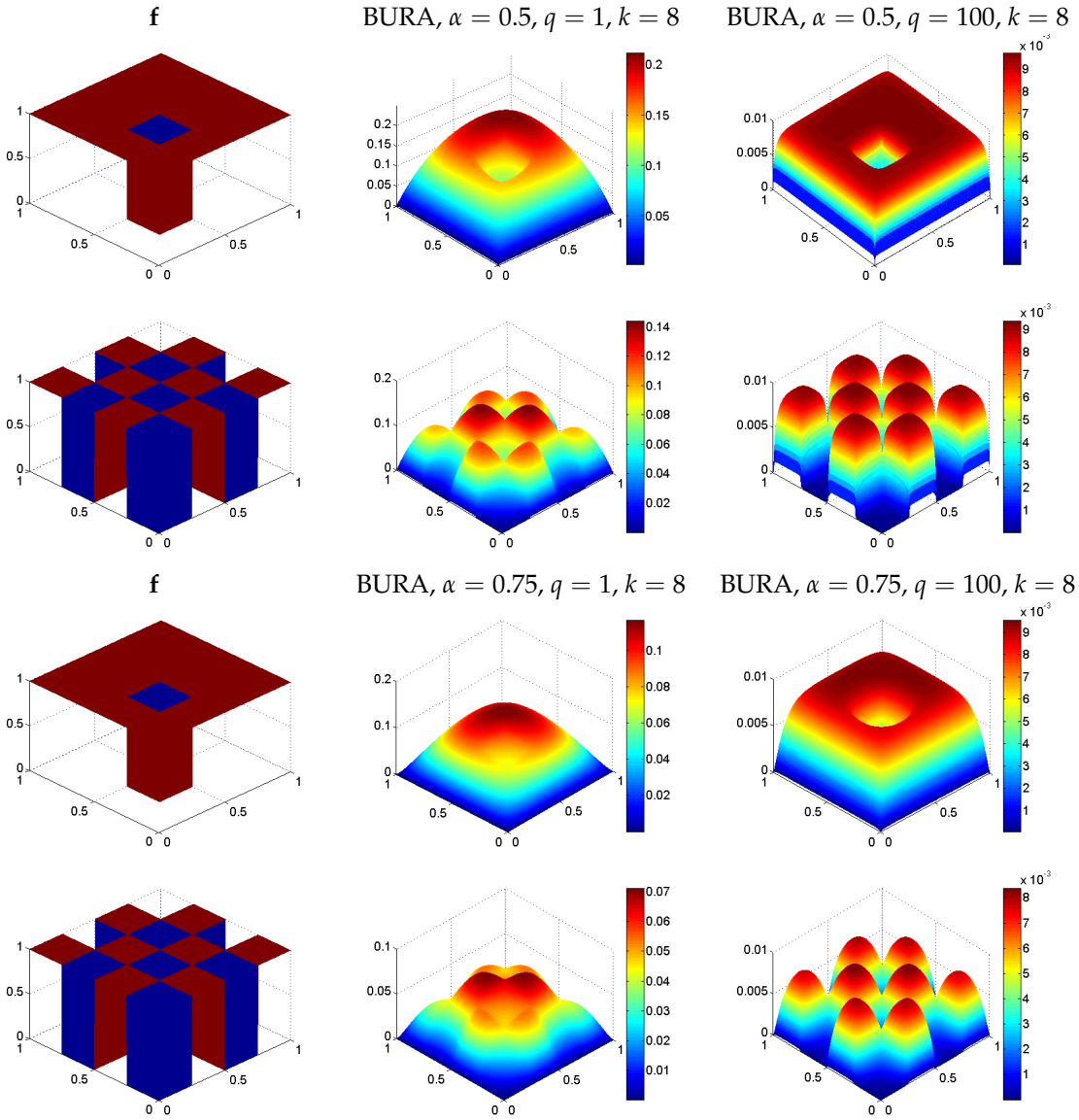


Figure 1. Numerical examples: The two choices for the right-hand-side of (5) and their corresponding BURA solutions $\mathbf{u}_8^{(2)}$, with respect to the indicated parameters α, q on $[h, 1-h] \times [h, 1-h]$, $h = 2^{-10}$.

We consider $\alpha \in \{0.50, 0.75\}$, $q \in \{1, 100\}$, and $k \in \{4, 8\}$. When $q = 1$, the diffusion effect of $\mathbb{A}^\alpha$ is well represented, as can be seen in the second column of Figure 1. When $q = 100$, the reaction term dominates and the shape of the solution resembles the shape of the right-hand side. This effect is further and further enhanced with the increment of q. Similar behaviour is observed when q is fixed and α decreases.

According to the theory, which has also been confirmed by numerical tests, the non-negativity preservation of URA is independent of k. As observed, this behavior is likewise confirmed experimentally by the BURA numerical tests.

For all considered setups, both URA and BURA numerical solutions are positive and well separated from zero. Actually, for all $3 \leq k \leq 8$ and both $\alpha \in \{0.5, 0.75\}$

$$\min \mathbf{u}_k^{(1,2)} = O\left(10^{-4}\right), \quad \mathbf{f} = \mathbf{f}_1,\ q = 1; \qquad \min \mathbf{u}_k^{(1,2)} = O\left(10^{-7}\right), \quad \mathbf{f} = \mathbf{f}_2,\ q = 1;$$
$$\min \mathbf{u}_k^{(1,2)} = O\left(10^{-5}\right), \quad \mathbf{f} = \mathbf{f}_1,\ q = 100; \qquad \min \mathbf{u}_k^{(1,2)} = O\left(10^{-9}\right), \quad \mathbf{f} = \mathbf{f}_2,\ q = 100.$$

The difference functions $\mathbf{u}_k^{(2)} - \mathbf{u}_k^{(1)}$ are plotted on Figure 2. The order of the magnitude of every difference function is smaller than the order of the magnitude of the corresponding BURA/URA solutions, which agrees with [21]. As expected, the largest difference values are around the discontinuities of the right-hand-side and the boundary condition–**f** values disagreements. As q increases, so does the above dependence and its visualization.

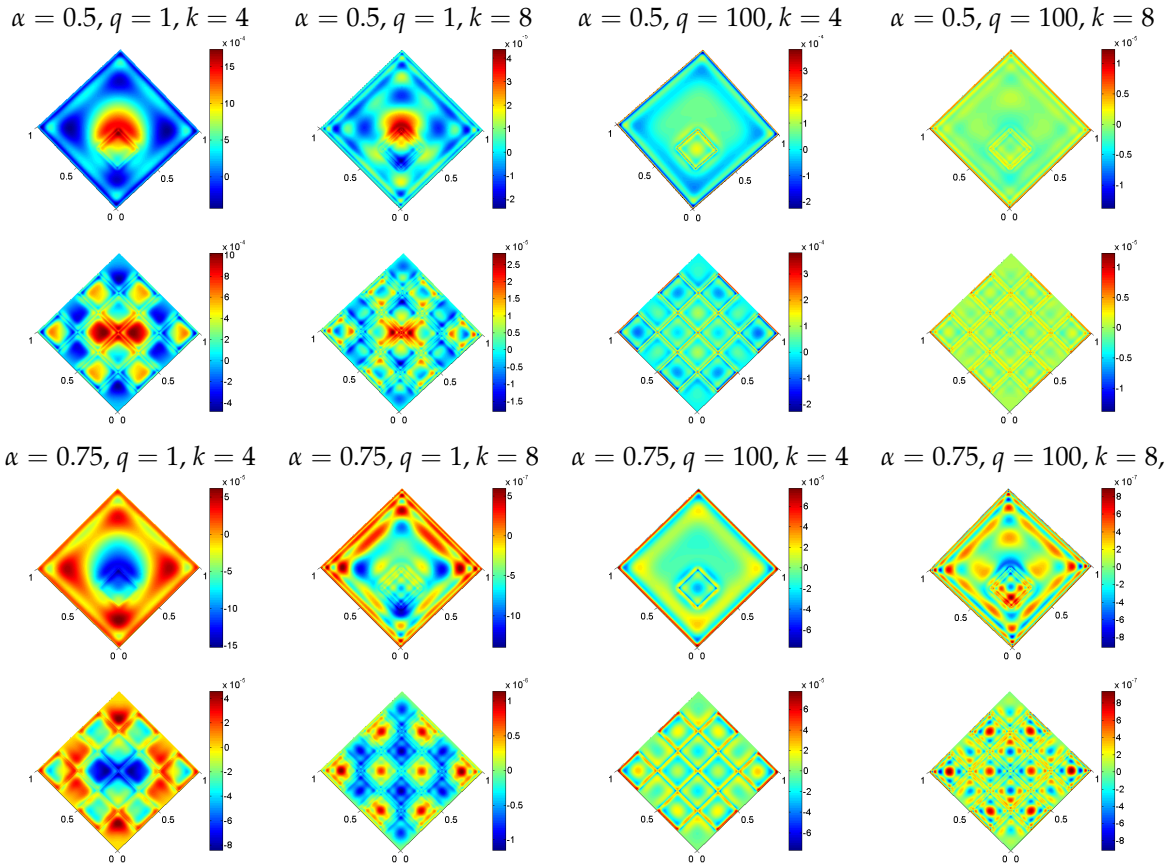


Figure 2. Numerical examples: Plots of the difference function $\mathbf{u}_k^{(2)} - \mathbf{u}_k^{(1)}$ for the considered choices of α, q, k. In each group, for $\alpha \in \{0.5, 0.75\}$, the first row of plots corresponds to f_1 and the second to f_2.

7. Discussion

This paper contains results that qualitatively and quantitatively characterize the spectral fractional diffusion–reaction problems. In short, the main contributions are identified by the presented systematic analysis. We show first that the maximum principle is valid in both the continuous and discrete cases, and then that the considered rational approximations of the BURA and URA type preserve the monotonicity of the numerical solution. It is well known that such a chain of properties is not unconditionally valid, for example, in the

non-fractional case. The fractional diffusion term makes the problem non-local, which generally complicates the analysis.

The theoretical results presented are based on assumptions, with the aim being to minimize the imposed requirements. For example, in Theorem 1, where the maximum principle is proven for fractional diffusion–reaction problems, there are no additional requirements compared to the non-fractional case. This is particularly case because the elliptic extension introduced in Lemma 1 is valid under most general assumptions. Both finite difference stencils and finite element meshes guarantee that the corresponding FDM matrix $\mathbb{A}$ and the FEM stiffness matrix $\mathbb{S}$ belong to the Stieltjes class. In the simpler case of standard (local) diffusion, this is sufficient to comply with the discrete maximum principle. We emphasize that this holds for the FEM discretization of the fractional diffusion equation if and only if the mass matrix is lumped. Then the BURA numerical solution of the corresponding dense linear systems preserves the monotonicity due to interlacing inequalities of roots and poles of the rational approximation of z^α. A more in-depth analysis was needed in the case of a fractional diffusion reaction, where the highest value contributions are also contained. Here, the URA and BURA numerical solutions have some complementary properties. Thus, the final result for preserving monotonicity (see Theorem 3) is obtained for the URA case. Consistent with theory, BURA outperforms URA in terms of accuracy, although both methods have an exponential convergence rate with respect to the power k. This is confirmed by numerical experiments. However, experimental results also show interlacing behaviour of the roots and poles of the best uniformly rational approximation of $g(z) = 1/(z^{-\alpha} + q)$. This led to the hypothesis that the monotonicity preservation statement from Theorem 3 also holds for the BURA method.

Theorem 1 plays a central role in the present analysis. It also raises the question of whether a maximum principle for fractional diffusion–reaction problems can hold for positive powers $\alpha \leq 0.5$. The proof of the theorem relies on the one-dimensional Sobolev embedding theorem, in which the L^∞ norm is controlled by the H^α norm. It is well known that this embedding holds only for $\alpha > 0.5$. Consequently, extending the proof of the maximum principle to smaller values of α would necessitate a fundamentally different analytical approach.

This article also addresses a number of new issues regarding the BURA and URA methods. Qualitatively, new constructive results have been obtained. These, in turn, lead to new challenges and open questions. Such examples are the following two specific questions for fractional diffusion–reaction problems: (a) proof of interlacing inequalities for the roots and poles of the best uniform rational approximation of $g(z)$, $z \in [0, 1]$; (b) improving the convergence of the URA and BURA methods by appropriate scaling in the definitions of the approximations $\mathbf{u}_k^{(1)}$ and $\mathbf{u}_k^{(2)}$.

Our future plans include research on questions related to the maximum principle for parabolic and convection–diffusion–reaction problems involving spectral fractional diffusion terms.

In conclusion, it appears significantly more challenging to obtain comparable results when the reaction coefficient $q(x) \geq 0$ is not a constant. For instance, the BURA framework, which relies on rational approximation of the scalar function $g(z) = 1/(z^{-\alpha} + q)$, is no longer applicable in the variable-coefficient case. Consequently, addressing this setting requires the development of a fundamentally new approach.

Author Contributions: Conceptualization, S.H. and S.M.; methodology, S.M.; software, S.H.; formal analysis, S.H. and S.M.; writing—original draft preparation, S.M.; writing—review and editing, S.H. and S.M.; visualization, S.H. All authors have read and agreed to the published version of the manuscript.

Funding: This work was partially supported by the Centre of Excellence in Informatics and ICT under the Grant No BG16RFPR002-1.014-0018-C01, financed by the Research, Innovation and Digitalization for Smart Transformation Programme 2021-2027 and co-financed by the European Union. The authors also acknowledge partial support by the Bulgarian National Science Fund under grant No. KP-06-N72/2.

Data Availability Statement: The numerical code used to support the findings of this study is not publicly available at present, as it is part of ongoing work and not yet suitable for public release. Methodological details intended to facilitate the independent development of scripts for reproducing the numerical experiments are provided in Appendix A.

Acknowledgments: The authors dedicate their research to the memory of Raytcho Lazarov.

Conflicts of Interest: The authors declare no conflicts of interest.

Appendix A. Computational Details to Section 6

In this section, we will provide additional details on the execution of our conducted numerical experiments in Section 6.2 in order to allow for the reproducibility of the results.

We applied BURA and URA numerical solvers to the problem (5), where, following Section 2.1, the matrix $\mathbb{A} \in \mathbb{R}^{N\times N}$, $N = n^2$, had the following block structure:

$$\mathbb{A} = \frac{1}{h^2}\begin{bmatrix} \mathbb{A}_{1,1} & -\mathbb{I} & & & \\ -\mathbb{I} & \mathbb{A}_{2,2} & -\mathbb{I} & & \\ \cdots & \cdots & \cdots & \cdots & \cdots \\ & -\mathbb{I} & \mathbb{A}_{i,i} & -\mathbb{I} & \\ \cdots & \cdots & \cdots & \cdots & \cdots \\ & & & -\mathbb{I} & \mathbb{A}_{n,n} \end{bmatrix}, \quad \mathbb{A}_{i,i} = \begin{bmatrix} 4 & -1 & & \\ -1 & 4 & -1 & \\ \cdots & \cdots & \cdots & \cdots \\ & -1 & 4 & -1 \\ & & -1 & 4 \end{bmatrix}.$$

Here, $\mathbb{A}_{i,i} \in \mathbb{R}^{n\times n}$, $i = 1, \cdots, n$ and $\mathbb{I}$ are the identity matrix in $\mathbb{R}^n$.

Problem (5) is the finite difference discretization of the fractional diffusion–reaction problem (3) with homogeneous Dirichlet boundary conditions, where $\mathcal{A} = -\Delta$ corresponds to the classical 2D Laplace operator. We only consider the FDM setting due to the equivalency between the former and the linear FEM discretization with a lumped mass matrix on structured grids. Since our computational domain $[0,1] \times [0,1]$ is a tensor product of unit intervals, we introduce the three-point stencil approximation of the 1D Laplace operator $\mathbb{B} \in \mathbb{R}^{n\times n}$, where $n = \frac{1}{h} - 1$

$$\mathbb{B} = \frac{1}{h^2}\begin{bmatrix} 2 & -1 & & \\ -1 & 2 & -1 & \\ \cdots & \cdots & \cdots & \cdots \\ & -1 & 2 & -1 \\ & & -1 & 2 \end{bmatrix}.$$

We have the identity $\mathbb{A} = \mathbb{B} \otimes \mathbb{I} + \mathbb{I} \otimes \mathbb{B}$, where $\otimes$ denotes the Kronecker product of matrices. The eigenvalues and normalized eigenvectors of $\mathbb{B}$ are, respectively,

$$\lambda_i = \frac{4}{h^2}\sin^2\left(\frac{i\pi h}{2}\right), \qquad \Psi_i = \sqrt{2h}\{\sin(ik\pi h)\}_{k=1}^{n}, \qquad i = 1, \ldots, n.$$

In particular,

$$\lambda_1 = \frac{4}{h^2}\sin^2\left(\frac{\pi h}{2}\right) \approx \frac{4}{h^2}\left(\frac{\pi h}{2}\right)^2 = \pi^2,$$

independently from the choice of $h \ll 1$.

Thus, the eigenvalues and normalized eigenvectors of $\mathbb{A}$ are

$$\lambda_{kl} = \frac{4}{h^2}\left(\sin^2\left(\frac{k\pi h}{2}\right) + \sin^2\left(\frac{l\pi h}{2}\right)\right), \qquad \mathbf{\Psi}_{kl} = \mathbf{\Psi}_k(x)\mathbf{\Psi}_l(y), \qquad k,l = 1,\ldots,n.$$

In particular, $\mu_1 = \lambda_{11} = 2\lambda_1 \approx 2\pi^2$.

The choice for $h = 2^{-10}$ is a balanced one. The mesh is not very fine; thus, the execution time for our algorithms is relatively low, but, at the same time, the mesh is not very coarse, either, giving rise to an approximately 10^{-3} discretization step in space, which is still practical for certain real-life applications. As mentioned in Section 6.2, such an h gives rise to $n = 2^{10} - 1 = 1023$ and $N = n^2 = 1046529$, respectively. We have conducted experiments with $k \in \{3,4,5,6,7,8\}$ for $\alpha \in \{0.50, 0.75\}$ and both considered right-hand sides $\{\mathbf{f}_1, \mathbf{f}_2\}$. Runtimes depend linearly on k when sequential algorithms are used, as we need to independently solve k linear systems on diagonal shifts of $\mathbb{A}$. We apply the Thomas algorithm with separation of variables for solving each of the diagonally shifted systems.

In summary, our experiments follow the following procedure:

1. For given $\{\alpha, q, k\}$, compute the coefficients $\{c_i\}$ and the poles $\{d_i\}$ of $r_{\alpha,k}(z)$ (URA) and $r_{\alpha,q,k}(z)$ (BURA), using BRASIL v2.1.0 software.
2. Apply the proof of Lemma 4 to compute the coefficients $\{\tilde{c}_i\}$ and the poles $\{\tilde{d}_i\}$ of $r_{\alpha,k}(z^{-1})$ and $r_{\alpha,q,k}(z^{-1})$.
3. Derive the corresponding fractional decomposition (16) and use $\mu_1 = 2\pi^2$ for scaling.
4. For each system of the type $(\mathbb{A} - \tilde{d}_i\mathbb{I})\mathbf{u} = \mathbf{f}$, apply the Thomas algorithm:
   - Construct $\mathbb{W} = (\mathbf{\Psi}_1^T, \mathbf{\Psi}_2^T, \ldots, \mathbf{\Psi}_n^T)$.
   - Compute $\mathbf{g}_i = \mathbb{W}^T\mathbf{f}_i$, $i = 1,\ldots,n$.
   - Construct $\mathbb{D} = diag(\lambda_i + 2/h^2)$ and compute

$$\left|\begin{array}{l} \mathbb{D}\mathbf{v}_1 - \mathbf{v}_2 = \mathbf{g}_1 \\ -\mathbf{v}_{i-1} + \mathbb{D}\mathbf{v}_i - \mathbf{v}_{i+1} = \mathbf{g}_i, \quad i = 2,\ldots,n-1 \\ -\mathbf{v}_{n-1} + \mathbb{D}\mathbf{v}_n = \mathbf{g}_n \end{array}\right.$$

   - Compute $\mathbf{u}_i = \mathbb{W}\mathbf{v}_i$, $i = 1,\ldots,n$.

Once we compute the corresponding BURA/URA numerical solution, we take min $\mathbf{u}$ to be the smallest value among its $n \times n$ entries.

References

1. Fraenkel, L. *An Introduction to Maximum Principles and Symmetry in Elliptic Problems*; Cambridge University Press: Cambridge, UK, 2008; Volume 128.
2. Ishihara, K. Strong and weak discrete maximum principles for matrices associated with elliptic problems. *Linear Algebra Appl.* **1987**, *88*, 431–448. [CrossRef]
3. Micchelli, C.A.; Willoughby, R.A. Functions which preserve the class of Stieltjes matrices. *Linear Algebra Appl.* **1979**, *3*, 141–156. [CrossRef]
4. Pucci, P.; Serrin, J. A note on the strong maximum principle for elliptic differential inequalities. *J. Math. Pures Appl.* **2000**, *79*, 57–71. [CrossRef]
5. Karátson, J.; Korotov, S.; Křížek, M. On discrete maximum principles for nonlinear elliptic problems. *Math. Comput. Simul.* **2007**, *76*, 99–108. [CrossRef]
6. Liska, R.; Shashkov, M. Enforcing the Discrete Maximum Principle for Linear Finite Element Solutions of Second-Order Elliptic Problems. *Commun. Comput. Phys.* **2008**, *3*, 852–877.
7. Vejchodský, T. The discrete maximum principle for Galerkin solutions of elliptic problems. *Cent. Eur. J. Math.* **2012**, *10*, 25–43. [CrossRef]
8. Caffarelli, L.; Silvestre, L. An Extension Problem Related to the Fractional Laplacian. *Commun. Partial. Differ. Equ.* **2007**, *32*, 1245–1260. [CrossRef]

9. Caffarelli, L.; Stinga, P. Fractional elliptic equations, Caccioppoli estimates and regularity. *Ann. l'Inst. Henri Poincarè C Anal. Linèaire* **2016** *33*, 767–807.
10. Ciarlet, P.; Raviart, P. Maximum principle and uniform convergence for the finite element method. *Comput. Method. Appl. Mech. Engrg.* **1973**, *1*, 17–31. [CrossRef]
11. Barrios, B.; Medina, M. Strong maximum principles for fractional elliptic and parabolic problems with mixed boundary conditions. *Proc. Roy. Soc. Edinburgh Sect.* **2020**, *150*, 475–495. [CrossRef]
12. Hofreither, C. A unified view of some numerical methods for fractional diffusion. *Comput. Math. Appl.* **2020**, *80*, 332–350. [CrossRef]
13. Harizanov, S.; Lazarov, R.; Margenov, S.; Marinov, P.; Vutov, Y. Optimal solvers for linear systems with fractional powers of sparse SPD matrices. *Numer. Linear Algebra Appl.* **2018**, *25*, e2167. [CrossRef]
14. Harizanov, S.; Lazarov, R.; Margenov, S.; Marinov, P.; Pasciak, J. Analysis of numerical methods for spectral fractional elliptic equations based on the best uniform rational approximation. *J. Comput. Phys.* **2020**, *408*, 109285. [CrossRef]
15. Harizanov, S.; Lazarov, R.; Margenov, S. A survey on numerical methods for spectral space-fractional diffusion problems. *Fract. Calc. Appl. Anal.* **2020**, *23*, 1605–1646. [CrossRef]
16. Kosturski, N.; Margenov, S. Analysis of BURA and BURA-based approximations of fractional powers of sparse SPD matrices. *Fract. Calc. Appl. Anal.* **2024**, *27*, 706–724. [CrossRef]
17. Margenov, S. Algebraic multilevel preconditioning in spectral fractional diffusion. *Appl. Math.* **2025**, *70*, 851–874. [CrossRef]
18. Hofreither, C. An algorithm for best rational approximation based on barycentric rational interpolation. *Numer. Algor* **2021**, *88*, 365–388. [CrossRef]
19. Software BRASIL. Available online: https://baryrat.readthedocs.io/en/latest/#baryrat.brasil (accessed on 21 January 2026).
20. Harizanov, S.; Margenov, S. Positive Approximations of the Inverse of Fractional Powers of SPD M-Matrices. In *Control Systems and Mathematical Methods in Economics, Lecture Notes in Economics and Mathematical Systems*; Feichtinger, G., Kovacevic, R., Tragler, G., Eds.; Springer International Publishing: Cham, Switzerland, 2018; Volume 687, pp. 147–163.
21. Harizanov, S.; Lazarov, R.; Margenov, S.; Marinov, P. Numerical solution of fractional diffusion-reaction problems based on BURA. *Comput. Math. Appl.* **2020**, *80*, 316–331. [CrossRef]
22. Nochetto, R.H.; Otárola, E.; Salgado, A.J. A PDE approach to space-time fractional parabolic problems. *SIAM J. Numer. Anal.* **2016**, *54*, 848–873. [CrossRef]
23. Salgado, A.J.; Sawyer, S.E. A Semi-Analytic Diagonalization FEM for the Spectral Fractional Laplacian. *arXiv* **2024**. [CrossRef]
24. Stahl, H. Best uniform rational approximation of x^{α} on $[0,1]$. *Bull. Am. Math. Soc. (New Ser.)* **1993**, *28*, 116–122. [CrossRef]

Disclaimer/Publisher's Note: The statements, opinions and data contained in all publications are solely those of the individual author(s) and contributor(s) and not of MDPI and/or the editor(s). MDPI and/or the editor(s) disclaim responsibility for any injury to people or property resulting from any ideas, methods, instructions or products referred to in the content.